

Theory of mixed classical-quantum scattering of molecules from surfaces

Ileana Ifimia and J. R. Manson

Department of Physics and Astronomy, Clemson University, Clemson, South Carolina 29634

(Received 24 July 2001; published 13 February 2002)

A theoretical model is developed for describing the scattering of molecules from surfaces, which includes energy and momentum transfers between the surface and projectile for both translational and rotational motion, and internal-mode excitation of the projectile molecule. The translational and rotational motions, including multiphonon excitations with the surface, are treated in the classical limit. Internal-vibrational-mode excitation of the molecules is treated quantum mechanically, with extension to arbitrary numbers of internal modes and arbitrary excitation quantum numbers. Examples of calculations are carried out for the surface scattering of a simple diatomic molecule.

DOI: 10.1103/PhysRevB.65.125401

PACS number(s): 34.50.Dy, 34.50.Pi, 82.20.Rp

I. INTRODUCTION

The scattering of molecules by surfaces is of significant current interest largely because of its relationship to the study of chemical reactions on substrates. However, molecular scattering is also capable of supplying a great deal of information on surface dynamics such as excitation of phonons, and other surface modes such as electron-hole pairs and surface plasmons. As opposed to the scattering of single atomic projectiles, molecules can interact with the surface via excitation or deexcitation of internal modes such as rotation and vibrations. Thus the molecule-surface interaction is significantly more complicated than the scattering of simple atoms, but it also holds forth the possibility of supplying much more interesting information.

In order to extract the maximum information possible from a scattering experiment, the measurement should be made state to state, i.e., an experiment in which the molecules in the beam are prepared in a well-defined translational, rotational, and vibrational state, and the detector measures the same properties of the scattered molecules. A number of recent experiments have achieved excellent state-to-state measurements for the scattering of light diatomic molecules such as H_2 and D_2 ,¹⁻³ other experiments have measured heavier diatomic molecule scattering⁴⁻⁸ and significant recent advances have been made in the scattering of larger molecules.⁹⁻¹²

In cases of scattering of light-mass molecules such as H_2 , a theoretical treatment of the scattering process must be completely quantum mechanical, even for describing the energy exchange with phonons at the surface,^{13,14} unless the incident translational energy is significantly more than 100 meV.¹⁵ At typical energies achieved with heavier molecular beams from hypersonic jet sources, classical physics is adequate to treat the translational and rotational motions. However, since internal molecular vibrational modes often have energies larger than 100 meV it is nearly always necessary to treat the vibrational excitations quantum mechanically.

The purpose of this paper is to develop a theoretical framework for describing the scattering of small molecules in the regime in which the rotational and translational motion can be treated classically, while treating the excitation of internal vibrational modes quantum mechanically. The treat-

ment of phonon transfers is handled using multiphonon theory that has been demonstrated to explain the inelastic scattering of heavier rare gases with up to several eV of translational energy, and also for He-atom scattering at energies above 100 meV. A classical treatment of rotational excitations is developed along lines similar to that for multiphonon excitations. The internal molecular vibrations are treated with a semiclassical theory within the harmonic approximation. The basic theoretical results for a single collision of the molecule with the surface can be expressed in terms of closed-form equations that are readily calculable. Calculations for scattering of a simple diatomic molecule are carried out in order to demonstrate the expected scattering spectra for angular distributions, rotational excitations, translational energy losses, and internal-mode excitation probabilities.

This paper is organized in the following manner. In the following section the general theory of molecular scattering is developed and several models are discussed for the exchange of phonons, for rotational excitations, and for the scattering form factor. Section III gives some representative calculations for CO scattering from a LiF(001) surface in order to demonstrate the results of this theory. In Sec. IV the results are discussed and some conclusions are drawn.

II. THEORY

A. General treatment

A starting point for describing molecular scattering from a many-body target is the state-to-state transition rate for an initial molecular projectile with well-defined translational momentum \mathbf{p}_i , angular momentum \mathbf{l}_i , and excitation quantum number q_{gi} for the g th mode, to a final state denoted by \mathbf{p}_f , \mathbf{l}_f , and q_{gf} . This is given by the generalized Fermi golden rule

$$w(\mathbf{p}_f, \mathbf{l}_f, q_{gf}, \mathbf{p}_i, \mathbf{l}_i, q_{gi}) = \left\langle \left\langle \frac{2\pi}{\hbar} \sum_{\{n_f\}} \left| T_{fi} \right|^2 \delta(\mathcal{E}_f - \mathcal{E}_i) \right\rangle \right\rangle, \quad (1)$$

where the average over initial translational and rotational states of the target crystal is denoted by $\langle \langle \rangle \rangle$, and the sum is over all unmeasured final states $\{n_f\}$ of the crystal that can

scatter a projectile into its specified final state. The energies \mathcal{E}_i and \mathcal{E}_f refer to the total energy of the system of projectile molecule plus the crystal before and after collision, respectively. The T_{fi} are the matrix elements of the transition operator \mathcal{T} taken with respect to unperturbed states of the system. The transition rate is the fundamental quantity for describing a scattering process, because all measurable quantities in a scattering experiment can be calculated from it.

In the semiclassical limit, the transition rate can be expressed as the Fourier transform over all times of a generalized time-dependent correlation function. In this same level of approximation, it is useful to assume that the elastic part of the interaction potential commutes with the inelastic part, and the transition rate is expressed as^{16,17}

$$w(\mathbf{p}_f, \mathbf{l}_f, q_{gf}, \mathbf{p}_i, \mathbf{l}_i, q_{gi}) = \frac{1}{\hbar^2} |\tau_{fi}|^2 \int_{-\infty}^{\infty} \exp[-i(E_f - E_i)t/\hbar] \times \exp[-2\mathcal{W}] \exp[\mathcal{Q}(t)] dt, \quad (2)$$

where $\exp[-2\mathcal{W}]$ is a generalized Debye-Waller factor and $\mathcal{Q}(t)$ is a generalized time-dependent correlation function. $|\tau_{fi}|^2$ is the scattering form factor, the square modulus of the off-energy-shell transition matrix of the elastic part of the interaction potential.

There can be several mechanisms for energy transfer in the collision process, such as phonons, rotational excitations, and internal mode excitations, all of which are considered here. If each of these processes is considered as independent, then the transition rate can be written in this separability limit as

$$w(\mathbf{p}_f, \mathbf{l}_f, q_{gf}, \mathbf{p}_i, \mathbf{l}_i, q_{gi}) = \frac{1}{\hbar^2} |\tau_{fi}|^2 \int_{-\infty}^{\infty} \exp[-i(E_f^T - E_i^T + E_f^R - E_i^R + E_f^V - E_i^V)t/\hbar] \times K_T(t, T_S) K_R(t, T_S) K_V(t, T_B) dt, \quad (3)$$

where $E_{f,i}^T$ is the translational energy of the final (f) or initial (i) projectile state, $E_{f,i}^R$ is the corresponding rotational energy of the projectile, and $E_{f,i}^V$ is the energy of the projectile's internal vibrational state. $K_T(t, T_S)$ is the scattering kernel for translational motion and phonon excitation, $K_R(t, T_S)$ is the scattering kernel for rotational excitation, and $K_V(t, T_B)$ is the kernel for internal-vibrational-mode excitation. Equation (3) is self-consistent in the following sense: although each of the three energy-exchange mechanisms is independent, each operates taking into consideration the energy losses or gains caused by the other mechanisms.

Starting from Eq. (3), the problem now becomes one of choosing models for the scattering kernels for each of the energy-exchange processes. For the interaction with phonons, an extension of the semiclassical model originally introduced by Bortolani and Levi and by Brako and Newns for inelastic scattering of ions and atoms from smooth sur-

faces will be applied.^{16,18,19} They showed that in the semiclassical limit the phonon-scattering kernel can be expressed in terms of a general exponentiated correlation function $Q_T(\mathbf{R}, t)$ as

$$K_T(t, T_S) = \int_{-\infty}^{\infty} d\mathbf{R} e^{i\mathbf{K} \cdot \mathbf{R}} e^{-2W_T(\mathbf{p}_f, \mathbf{p}_i)} e^{Q_T(\mathbf{R}, t)}, \quad (4)$$

where $2W_T(\mathbf{p}_f, \mathbf{p}_i) = Q_T(\mathbf{R}=0, t=0)$ is the contribution to the total Debye-Waller factor due to phonon exchange.

If the semiclassical limit is now extended to the limit of rapid collisions in which the semiclassical force exerted on the scattering particle can be replaced by the momentum impulse, then the correlation function simplifies to the time-dependent displacement-correlation function

$$Q_T(\mathbf{R}, t) = \langle \mathbf{p} \cdot \mathbf{u}(0,0) \mathbf{p} \cdot \mathbf{u}(\mathbf{R}, t) \rangle / \hbar^2, \quad (5)$$

where $\mathbf{u}(\mathbf{R}, t)$ is the phonon displacement at the position \mathbf{R} on the surface and $\mathbf{p} = \mathbf{p}_f - \mathbf{p}_i$ is the linear-momentum transfer. The argument of the Debye-Waller factor is given by the standard form, which for T_S greater than the Debye temperature Θ_D is

$$W_T(\mathbf{p}_f, \mathbf{p}_i) = \frac{3p^2 T_S}{2M_C k_B \Theta_D^2}, \quad (6)$$

where k_B is Boltzmann's constant and M_C is the crystal mass.

The classical limit of multiple-phonon exchange is obtained from Eq. (5) by making an expansion over small times and small position vectors around the point of collision, leading to

$$\langle \mathbf{p} \cdot \mathbf{u}(0,0) \mathbf{p} \cdot \mathbf{u}(\mathbf{R}, t) \rangle / \hbar^2 = 2W_T(\mathbf{p}_f, \mathbf{p}_i) - \frac{i}{\hbar} t \Delta E_0 - \frac{t^2}{\hbar^2} \Delta E_0 k_B T_S - \frac{\Delta E_0 k_B T_S R^2}{2\hbar^2 v_R^2}, \quad (7)$$

where $\Delta E_0 = \mathbf{p}^2 / 2M_C$ is the translational recoil energy and v_R is a weighted average over phonon velocities parallel to the surface.¹⁹

If phonons are the only mechanism for energy transfer, such as in atom scattering, then the scattering kernel of Eqs. (4)–(7) leads to a transition rate that is Gaussian-like in both the translational-energy transfer $E_f^T - E_i^T$ and the parallel component \mathbf{P} of the momentum transfer^{18,20,21}

$$w(\mathbf{p}_f, \mathbf{p}_i) = \frac{2\hbar v_R^2}{S_{u.c.}} |\tau_{fi}|^2 \left(\frac{\pi}{k_B T_S \Delta E_0} \right)^{3/2} \times \exp \left\{ - \frac{(E_f^T - E_i^T + \Delta E_0)^2 + 2v_R^2 P^2}{4k_B T_S \Delta E_0} \right\}. \quad (8)$$

This is the smooth-surface-scattering model for classical multiphonon transfers in an atom-surface collision. It takes into account the broken symmetry in the perpendicular direction caused by the presence of the surface, i.e., for every phonon exchanged only momentum parallel to the surface is

conserved. The perpendicular momentum exchange is not conserved as a consequence of the broken symmetry in that direction. The Debye-Waller factors, normally present in quantum-mechanical theory, have disappeared because they were canceled by the first term in Eq. (7) leaving the Gaussian-like behavior with an envelope factor that varies as the negative 3/2 power of the recoil and surface temperature.

There are also other classical expressions for describing classical multiphonon exchange. If the surface is regarded as a collection of isolated scattering centers in thermodynamic equilibrium, then the scattering kernel in the classical limit becomes simpler than Eq. (7),

$$K_T(t, T_S) = \exp \left\{ -\frac{i}{\hbar} t \Delta E_0 - \frac{t^2}{\hbar^2} \Delta E_0 k_B T_S \right\}, \quad (9)$$

which leads to another Gaussian-like expression for the transition rate for atomic scattering given by

$$w(\mathbf{p}_f, \mathbf{p}_i) = \frac{1}{\hbar} |\tau_{fi}|^2 \left(\frac{\pi}{k_B T_S \Delta E_0} \right)^{1/2} \times \exp \left\{ -\frac{(E_f^T - E_i^T + \Delta E_0)^2}{4k_B T_S \Delta E_0} \right\}. \quad (10)$$

This is the discrete model for atomic scattering and it differs from Eq. (8) in that the Gaussian-like factor in \mathbf{P}^2 is absent and the envelope function varies only as the $-1/2$ power of the temperature rather than the $-3/2$ power. The physical difference between the two expressions of Eqs. (8) and (10) is the corrugation of the surface. Equation (8) describes a surface that is smooth except for the vibrational corrugations caused by the time-dependent motions of the underlying atoms, while Eq. (10) describes a surface that is highly corrugated, so highly corrugated that each scattering center is distinct. Other models for the classical-multiphonon limit have been proposed for surfaces that are corrugated in a manner intermediate between these two extreme limits.²² These intermediate models all have the common feature of Gaussian-like behavior in energy transfer, and show that the corrugation of the surface can be directly related to the temperature and recoil-energy dependence of the envelope factor. These expressions of Eqs. (8) and (10), when extended to include multiple collisions with the surface, have been demonstrated to explain the scattering of rare-gas atoms^{23,24} and low-energy ions²⁵ from a variety of surfaces.

The next task is to develop a scattering kernel for the rotational motion of the molecular projectile. In order to be consistent with the smooth-surface model of Eq. (7) for the translational motion, a model is developed that preserves the correct angular momentum conservation for a rotating molecule interacting with a smooth surface, i.e., angular momentum will be conserved in the direction perpendicular to the surface but not in the directions parallel to the surface. Starting from Eq. (1) in the semiclassical limit, but with the proper angular momentum conservation for a smooth surface, the scattering kernel for rotational motion is²⁶

$$K_R(t, T_S) = \int_{-\infty}^{\infty} d\theta_z e^{i l_z \theta_z / \hbar} e^{-2W_R(\mathbf{l}_f, \mathbf{l}_i)} e^{Q_R(\theta_z, t)}, \quad (11)$$

where $\mathbf{l}_{i,f}$ are, respectively, the final and initial angular momenta of the molecule, $\mathbf{l} = \mathbf{l}_f - \mathbf{l}_i$ is the angular momentum transfer, $Q_R(\theta_z, t)$ is a generalized rotational-correlation function, and the rotational contribution to the Debye-Waller factor is $2W_R(\mathbf{l}_f, \mathbf{l}_i) = Q_R(\theta_z = 0, t = 0)$. In the limit of a quick collision, where the angular forces are given by the angular impulse, the correlation function becomes a correlation function of the angular displacement $\Theta(\theta_z, t)$,

$$Q_R(\theta_z, t) = \langle \mathbf{l} \cdot \Theta(0, 0) \mathbf{l} \cdot \Theta(\theta_z, t) \rangle / \hbar^2. \quad (12)$$

At this point, the calculation of the angular-scattering kernel is still fully quantum mechanical, although it is in the semiclassical limit. The extension to the classical limit of exchange of large numbers of rotational quanta is again similar to Eq. (7),

$$\begin{aligned} & \langle \mathbf{l} \cdot \Theta(0, 0) \mathbf{l} \cdot \Theta(\theta_z, t) \rangle / \hbar^2 \\ &= 2W_R(\mathbf{l}_f, \mathbf{l}_i) - \frac{i}{\hbar} t \Delta E_0^R - \frac{t^2}{\hbar^2} \Delta E_0^R k_B T_S - \frac{\Delta E_0^R k_B T_S \theta_z^2}{2\hbar^2 \omega_R^2}, \end{aligned} \quad (13)$$

where $\Delta E_0^R = l_x^2/2I_{xx}^c + l_y^2/2I_{yy}^c + l_z^2/2I_{zz}^c$ is the rotational recoil energy, the $I_{xx,yy,zz}^c$ are the principal moments of inertia of a surface molecule, and ω_R is a weighted average of frustrated rotational angular velocities of the surface molecules in the z direction. The constant ω_R plays a similar role for rotational transfers as the weighted average of parallel phonon velocities v_R in Eq. (8). Both of these quantities can be computed if the complete dynamical structure function of the surface is known. For the purpose of this work, these quantities will be treated as parameters. The principal moments I_{ii}^c are normally expected to be those of a surface molecule in the case of a molecular target. However, if the projectile molecules are large and strike more than one surface molecule simultaneously, then I_{ii}^c is expected to become an effective moment of inertia, larger than that of a single molecule. In the case of monatomic solids, an effective surface molecule consisting of two or more surface atoms must be chosen. In either case, the product $\omega_R^2 I_{ii}^c$ can be regarded as an alternative choice of the parameter ω_R .

The remaining task is to include in the transition rate the contributions from vibrational excitations of the internal modes of the molecular projectile. If these modes are treated in the harmonic limit, and consistently with the semiclassical approximations used in obtaining the translational and rotational scattering kernels, the problem becomes that of a collection of forced harmonic oscillators.²⁷ The general result has been worked out for the case of surface scattering,²⁸ and the internal-mode scattering kernel can be written in the following form:

$$\begin{aligned}
K_V(t, T_B) = & \sum_{\kappa, \kappa'=1}^{N_A} \{ \exp[i(\mathbf{p}_f \cdot \Delta \mathbf{r}_{\kappa, \kappa'}^f - \mathbf{p}_i \cdot \Delta \mathbf{r}_{\kappa, \kappa'}^i) / \hbar] \\
& \times \exp[-W_{V, \kappa}^p(\mathbf{p}_f, \mathbf{p}_i)] \\
& \times \exp[-W_{V, \kappa'}^p(\mathbf{p}_f, \mathbf{p}_i)] \exp[Q_{V, \kappa, \kappa'}^p(\mathbf{p}_f, \mathbf{p}_i, t)] \}, \\
\end{aligned} \tag{14}$$

where N_A is the number of atoms in the molecule and m_κ is the mass of the κ th molecular atom. The position of the κ th atom of the molecule just before the collision (i) or just after (f) is given by $\mathbf{r}_\kappa^i(t) = \mathbf{r}_\kappa^i + \mathbf{u}_\kappa^i(t)$ so that, for example, $\Delta \mathbf{r}_{\kappa, \kappa'}^f = \mathbf{r}_\kappa^f - \mathbf{r}_{\kappa'}^f$. The vibrational displacement relative to \mathbf{r}_κ^i due to the internal mode, decomposed into cartesian components denoted by β , is

$$u_\kappa^\beta(t) = \sum_{j=1}^{N_\nu} \sqrt{\frac{\hbar}{2N_\nu m_\kappa \omega_j}} e^{(j|\beta)} [a_j e^{-i\omega_j t} + a_j^\dagger e^{i\omega_j t}], \tag{15}$$

where N_ν is the total number of internal modes, a_j and a_j^\dagger are, respectively, the annihilation and creation operators for the j th mode of frequency ω_j , and $e^{(j|\beta)}$ is the polarization vector that is obtained from a normal modes analysis of the molecule.

The displacement-correlation function for internal bending modes of the projectile molecule is then written as

$$\begin{aligned}
Q_{V, \kappa, \kappa'}^p(\mathbf{p}_f, \mathbf{p}_i, t) &= \sum_{\alpha, \alpha'=1}^3 p_\alpha p_{\alpha'} \sum_{j=1}^{N_\nu} \frac{1}{2N_\nu \hbar \sqrt{m_\kappa m_{\kappa'} \omega_j}} e^{(j|\alpha)} e^{*(j'|\alpha')} \\
&\times \{ n(\omega_j) e^{i\omega_j t} + [n(\omega_j) + 1] e^{-i\omega_j t} \}, \\
\end{aligned} \tag{16}$$

where $n(\omega_j)$ is the Bose-Einstein function, and the Debye-Waller factor associated with the κ th atom of the projectile

molecule becomes

$$W_{V, \kappa}^p(\mathbf{p}_f, \mathbf{p}_i) = \frac{1}{2} Q_{V, \kappa = \kappa'}^p(\mathbf{p}_f, \mathbf{p}_i, t=0). \tag{17}$$

In the internal-mode correlation function $Q_{V, \kappa, \kappa'}^p(\mathbf{p}_f, \mathbf{p}_i, t)$ the orthogonal modes commute with each other, and Eq. (16) can be further expanded to²⁹

$$\begin{aligned}
e^{Q_{V, \kappa, \kappa'}^p(\mathbf{p}_f, \mathbf{p}_i, t)} &= e^{\sum_{j=1}^{N_\nu} Q_{j, \kappa, \kappa'}^p(\mathbf{p}_f, \mathbf{p}_i, t)} \\
&= \prod_{j=1}^{N_\nu} \sum_{\alpha_j=-\infty}^{\infty} \left\{ I_{|\alpha_j|}(b_{\kappa, \kappa'}(\omega_j)) \right. \\
&\quad \left. \times \left[\frac{n(\omega_j) + 1}{n(\omega_j)} \right]^{\alpha_j/2} e^{-i\alpha_j \omega_j t} \right\}, \\
\end{aligned} \tag{18}$$

where $I_{|\alpha_j|}(z)$ is the modified Bessel function of integer order α_j and argument z . The argument of the modified Bessel function of Eq. (18) is given by

$$\begin{aligned}
b_{\kappa, \kappa'}(\omega_j) &= \sum_{\alpha, \alpha'=1}^3 p_\alpha p_{\alpha'} \frac{1}{N_\nu \hbar \sqrt{m_\kappa m_{\kappa'} \omega_j}} \\
&\times e^{(j|\alpha)} e^{*(j'|\alpha')} \sqrt{n(\omega_j) [n(\omega_j) + 1]}. \\
\end{aligned} \tag{19}$$

Equations (14)–(19) define the scattering kernel for excitation of internal molecular modes.

The three scattering kernels for translation, rotation, and internal vibrations can now be inserted back into Eq. (3) and all integrals can be readily carried out. The general result for the state-to-state transition rate is

$$\begin{aligned}
w(\mathbf{p}_f, \mathbf{l}_f, \mathbf{p}_i, \mathbf{l}_i) &= \frac{1}{\hbar^2} |\tau_{fi}|^2 \left(\frac{2\pi \hbar^2 v_R^2}{\Delta E_0 k_B T_S} \right) \left(\frac{2\pi \hbar^2 \omega_R^2}{\Delta E_0^R k_B T_S} \right)^{1/2} \left(\frac{\pi \hbar^2}{(\Delta E_0 + \Delta E_0^R) k_B T_S} \right)^{1/2} \exp \left[-\frac{2\mathbf{P}^2 v_R^2}{4\Delta E_0 k_B T_S} \right] \exp \left[-\frac{2l_z^2 \omega_R^2}{4\Delta E_0^R k_B T_S} \right] \\
&\times \sum_{\kappa, \kappa'=1}^{N_A} \left\{ \exp[i(\mathbf{p}_f \cdot \Delta \mathbf{r}_{\kappa, \kappa'}^f - \mathbf{p}_i \cdot \Delta \mathbf{r}_{\kappa, \kappa'}^i) / \hbar] \right. \\
&\times \exp[-W_{V, \kappa}^p(\mathbf{p}_f, \mathbf{p}_i)] \exp[-W_{V, \kappa'}^p(\mathbf{p}_f, \mathbf{p}_i)] \prod_{j=1}^{N_\nu} \sum_{\alpha_j=-\infty}^{\infty} I_{|\alpha_j|}(b_{\kappa, \kappa'}(\omega_j)) \\
&\quad \left. \times \left[\frac{n(\omega_j) + 1}{n(\omega_j)} \right]^{\alpha_j/2} \exp \left[-\frac{\left(E_f^T - E_i^T + E_f^R - E_i^R + \Delta E_0 + \Delta E_0^R + \hbar \sum_{s=1}^{N_\nu} \alpha_s \omega_s \right)^2}{4(\Delta E_0 + \Delta E_0^R) k_B T_S} \right] \right\}. \\
\end{aligned} \tag{20}$$

The transition rate of Eq. (20) is actually expressed, for compactness, as a product over all normal modes labeled by j and a summation over the excitation quantum number denoted by α_j . To obtain the discrete transition rate to a particular internal-mode final state or combination of states, one takes the corresponding (j, α_j) th term of Eq. (20).

The result of Eq. (20) retains many of the features of the simpler expressions of Eqs. (8) and (10) for atomic scattering with the exchange of only phonons. The dominant feature is the Gaussian-like function containing the three different modes of energy exchange (phonons, rotations, and internal molecular vibrations) together with the recoil terms from phonons ΔE_0 and from rotational exchange ΔE_0^R . The width of the Gaussian-like function varies as the square root of the temperature and the sum of the two recoil energies. This is not a true Gaussian because of the momentum dependencies of the recoil energies. There are also Gaussian-like functions in the exchange of parallel momentum \mathbf{P} and perpendicular angular momentum l_z that arise from retaining the correct momentum conservation conditions for a smooth surface. The envelope factors vary as negative powers of the temperature multiplied by recoil energies. These envelope factors guarantee the overall unitarity of the total scattered intensity, i.e., as the temperature and/or incident energy is increased, the maximum intensity of the Gaussian-like function decreases in order that the total integral over final states remains constant.

In Eq. (20) the quantum behavior of the internal-mode excitations is expressed differently than the classical behavior for translational and rotational motion. The strength of the α_j quantum excitation of the j th mode is proportional to the modified Bessel function $I_{|\alpha_j|}(b_{\kappa,\kappa'}(\omega_j))$. Because these are quantum features the vibrational contribution to the Debye-Waller factor is still present, as are quantum phase factors involving the positions \mathbf{r}_κ of the individual molecular atoms before and after the collision. The presence of these quantum phase factors can cause interference effects, but because in an actual experiment the orientation of a molecule is not measured, the transition rate must be averaged over molecular orientations in order to compare directly with experiments. Recoil effects due to the excitation of internal modes are not explicitly apparent in Eq. (20), but they are included within the modified Bessel function.

In many cases, such as where the incident molecular energy and the surface temperature are not large compared to the energy of internal-molecular-vibrational excitations, the expansion of Eq. (20) to only single quantum excitations is sufficient. This expansion is

$$\begin{aligned}
w(\mathbf{p}_f, \mathbf{l}_f, \mathbf{p}_i, \mathbf{l}_i) = & \frac{1}{\hbar^2} |\tau_{fi}|^2 \left(\frac{\pi \hbar^2}{(\Delta E_0 + \Delta E_0^R) k_B T_S} \right)^{1/2} \left(\frac{2 \pi \hbar^2 v_R^2}{\Delta E_0 k_B T_S} \right) \left(\frac{2 \pi \hbar^2 \omega_R^2}{\Delta E_0^R k_B T_S} \right)^{1/2} \exp \left[- \frac{2 \mathbf{P}^2 v_R^2}{4 \Delta E_0 k_B T_S} \right] \\
& \times \exp \left[- \frac{2 l_z^2 \omega_R^2}{4 \Delta E_0^R k_B T_S} \right] \sum_{\kappa, \kappa'=1}^{N_A} \exp [i(\mathbf{p}_f \cdot \Delta \mathbf{r}_{\kappa, \kappa'}^f - \mathbf{p}_i \cdot \Delta \mathbf{r}_{\kappa, \kappa'}^i) / \hbar] \exp [-W_{V, \kappa}^p(\mathbf{p}_f, \mathbf{p}_i)] \exp [-W_{V, \kappa'}^p(\mathbf{p}_f, \mathbf{p}_i)] \\
& \times \left\{ \exp \left[- \frac{(E_f^T - E_i^T + E_f^R - E_i^R + \Delta E_0 + \Delta E_0^R)^2}{4(\Delta E_0 + \Delta E_0^R) k_B T_S} \right] + \sum_{\gamma, \gamma'=1}^3 p_\gamma p_{\gamma'} \sum_{j=1}^{N_\nu} \frac{1}{2 \hbar N_\nu \sqrt{m_\kappa m_{\kappa'}} \omega_j} e^{(j|\gamma)} e^{*(j'|\gamma')} \right. \\
& \times \left(n(\omega_j) \exp \left[- \frac{(E_f^T - E_i^T + E_f^R - E_i^R + \Delta E_0 + \Delta E_0^R - \hbar \omega_j)^2}{4(\Delta E_0 + \Delta E_0^R) k_B T_S} \right] + [n(\omega_j) + 1] \right. \\
& \left. \left. \times \exp \left[- \frac{(E_f^T - E_i^T + E_f^R - E_i^R + \Delta E_0 + \Delta E_0^R + \hbar \omega_j)^2}{4(\Delta E_0 + \Delta E_0^R) k_B T_S} \right] \right) \right\}. \tag{21}
\end{aligned}$$

Of the three terms in Eq. (21) the one proportional to $n(\omega_j) + 1$ gives the single quantum creation rate, the term proportional to $n(\omega_j)$ is for single quantum annihilation, and the third term is the rate for scattering with no internal-mode creation.

B. The attractive potential well

The Van der Waals force between the surface and the incident molecular projectile gives rise to an attractive well in front of the surface that can have important effects at low incident translational energies, and can also affect the rotational excitations. In the case of classical scattering, the main effect of the Van der Waals attractive potential is to enhance the energy of the incoming particle associated with the direction normal to the surface. This is a refractive effect quite

similar to that which occurs for light waves in optically refractive media. Since refraction is the dominant effect, the potential can be modeled by a one-dimensional potential well, and for a given well depth $|D|$ the refraction does not depend on the functional shape of the attractive part of the potential. Thus, this attractive force can be simulated by an attractive one-dimensional square-well potential in front of the repulsive barrier, and the width of the well is unimportant. The effect of the collision process is to replace the perpendicular component of the momentum p_{qz} near the surface by a larger value p'_{qz} , which includes the well depth D

$$p'^2_{qz} = p^2_{qz} + 2m|D|. \tag{22}$$

This refracts all projectiles at the leading edge of the well and causes them to collide with a barrier with a higher nor-

mal energy. The expressions for projectile translational energy and for scattering angle inside of the potential well become, respectively,

$$E'_{f,i} = E_{f,i}^T + |D| \quad (23)$$

and

$$\cos(\theta'_f) = \left(\frac{E_f^T \cos^2(\theta_f) + |D|}{E_f^T + |D|} \right)^{1/2}. \quad (24)$$

Transition rates calculated for molecular scattering inside the well can then be projected to the asymptotic region outside the well by multiplication with an appropriate Jacobian function, which can be easily determined from Eqs. (23) and (24).

C. The scattering form factor

The scattering form factor $|\tau_{fi}|^2$ appearing as a multiplicative factor in the transition rate has not yet been specified. In the semiclassical limit of interest here τ_{fi} has been identified as the transition matrix for inelastic scattering, calculated from the elastic part of the potential, i.e., the transition rate for the elastic Hamiltonian extended off of the energy shell.¹⁷ A very useful expression, first applied to atom scattering, is the function suggested by the distorted-wave Born approximation for an exponentially repulsive surface barrier potential³⁰

$$V^0(z) = V_0 e^{-\beta z}. \quad (25)$$

This is given by the product of the Jackson-Mott matrix element in perpendicular momentum and a cutoff function in parallel momentum³⁰

$$|\tau_{fi}|^2 = |v_{J-M}(p_{fz}, p_{iz})|^2 e^{-\mathbf{P}^2/P_0^2}. \quad (26)$$

The Jackson-Mott matrix element $v_{J-M}(p_{fz}, p_{iz})$ is the matrix element of Eq. (25) taken with respect to its own distorted Schrödinger-equation eigenstate. It depends on only the perpendicular component of the momentum. Defining $q_i = p_{iz}/\hbar\beta$ and $q_f = p_{fz}/\hbar\beta$, it is given by

$$v_{J-M}(p_{fz}, p_{iz}) = \frac{\hbar^2 \beta^2}{m} \frac{\pi q_i q_f (q_f^2 - q_i^2)}{\cosh(\pi q_f) - \cosh(\pi q_i)} \times \left(\frac{\sinh(\pi q_f) \sinh(\pi q_i)}{q_i q_f} \right)^{1/2}. \quad (27)$$

In the semiclassical limit of a very hard repulsive surface (or an infinitely hard repulsive wall), $\beta \rightarrow \infty$, the Jackson-Mott matrix element as well as matrix elements for other one-dimensional potentials with a hard repulsive part, become

$$v_{J-M}(p_{fz}, p_{iz}) \rightarrow 2p_{fz} p_{iz} / m \quad (28)$$

and $P_0 \rightarrow \infty$. Thus the cutoff function goes to unity in the semiclassical limit, and the expression for the form factor reduces to simply the Jackson-Mott matrix element. This form factor has been successfully used to analyze atom-surface scattering in the classical limit, and has been used in

an earlier attempt to describe molecular scattering with rigid molecules.³¹ This is the expression that will be used in the calculations reported in Sec. III below.

D. Measurable quantities

The remaining task is to connect the transition rate of Eq. (1) to quantities that can be measured in actual experiments. The experimental quantity usually measured in a scattering process is the differential reflection coefficient $d^3R/d\Omega_f dE_f^T$ giving the fraction of the incident particles that are scattered into a final solid angle of the detector $d\Omega_f$, and into energy interval dE_f^T centered at E_f^T . This is proportional to the transition rate shown in Eqs. (20) and (21) and is obtained by dividing by the incident flux crossing a plane parallel to the surface, $j_i = p_{iz}/mL$, where L is a quantization length, and multiplying by the density of available final particle states

$$\frac{d^3R}{d\Omega_f dE_f^T}(\mathbf{p}_f, \mathbf{l}_f, \mathbf{p}_i, \mathbf{l}_i) = \frac{L^4}{(2\pi\hbar)^3} \frac{m^2 |\mathbf{p}_f|}{p_{iz}} w(\mathbf{p}_f, \mathbf{l}_f, \mathbf{p}_i, \mathbf{l}_i). \quad (29)$$

Some experiments use a detector, which is velocity dependent, and thus the differential reflection coefficient must be multiplied by a detector correction. The most common of these corrections is for the time-of-flight density detector whose sensitivity varies inversely with the speed of the particles passing through it. In this case the detector correction to be applied to Eq. (29) is to multiply the right-hand side by a factor of $1/v_{f\infty} 1/p_f$.

In a typical experiment, the incoming beam of molecules usually can be considered to have a well-defined translational energy and angular spread. However, normally the rotational state will be a distribution, which will be denoted by $P(\mathbf{l}_i, T_{iR})$, usually assumed to be a Maxwell-Boltzmann distribution at temperature T_{iR} and often with a temperature lower than that of the gas reservoir from which the hypersonic jet beam was produced. In this case, the differential reflection coefficient of Eq. (29) must be averaged over this distribution of incident rotational angular momenta. The translational energy distribution at a fixed final angle (the differential reflection coefficient) is then obtained from Eq. (29) by performing the averages and sums over all unmeasured degrees of freedom and is given by

$$\frac{d^3R}{d\Omega_f dE_f^T} = \left\langle \int d\mathbf{l}_i P(\mathbf{l}_i, T_{iR}) \int d\mathbf{l}_f \frac{d^3R}{d\Omega_f dE_f^T}(\mathbf{p}_f, \mathbf{l}_f, \mathbf{p}_i, \mathbf{l}_i) \right\rangle_R, \quad (30)$$

where $\langle \rangle_R$ refers to an average over all orientations of the initial and final angular momenta of the projectile molecule.

The angular distribution of scattered projectiles, summed over all rotational and internal-vibrational states is then obtained by summing Eq. (30) over all final translational energies

$$\frac{d^2R}{d\Omega_f} = \int_0^\infty dE_f^T \left(\frac{d^3R}{d\Omega_f dE_f^T} \right). \quad (31)$$

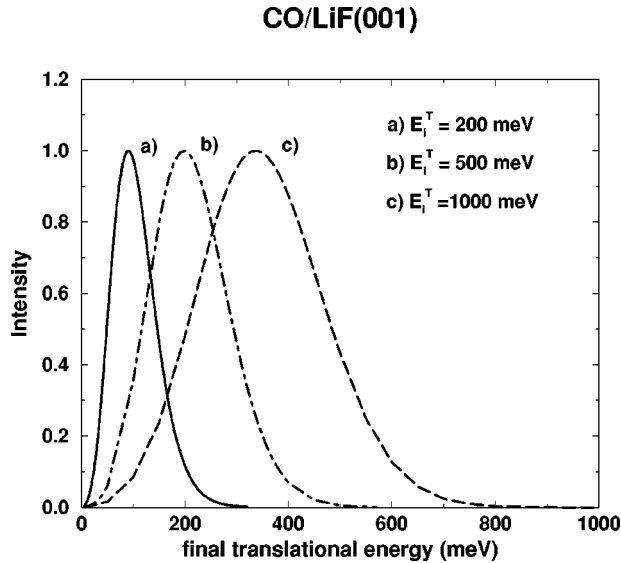


FIG. 1. Translational energy-resolved spectra for CO scattering from LiF(001). The initial angle $\theta_i = 45^\circ$ and the final angle is, for each incident energy, the position of the maximum in the angular distribution. The differential reflection coefficient of Eq. (30) is plotted as a function of the final translational energy for three different incident energies, as shown.

In a similar manner, and with appropriate averaging over degrees of freedom not measured, the results of all possible experiments can be compared with the differential reflection coefficient of Eq. (29). Also, Eq. (29) can be used as a distribution function for determining averages and moments of observable quantities, such as, average rotational energies, fractional internal-mode excitation probabilities, etc. Several examples of calculations are shown in the following section.

III. MODEL CALCULATIONS

In this section several examples of calculations for the scattering of a simple diatomic molecule are presented. The model chosen is CO scattering from the alkali halide insulator surface LiF(001).

A. Translational energy-resolved spectra

Figure 1 shows the energy-resolved spectrum as a function of the final translational energy. Three different incident energies E_i^T , 200, 500, and 1000 meV are shown. Specifically, what is plotted in Fig. 1 is the differential reflection coefficient of Eq. (30) as a function of the final translational energy. The incident angle was chosen to be $\theta_i = 45^\circ$ and the final angle is taken at the position of the maximum in the corresponding angular distributions calculated for the same incident energies and shown in Fig. 2 below.

The fixed input parameters needed in this calculation are the masses and moments of inertia of both CO and LiF, and for these the known atomic masses and interatomic distances were used.³² In the present calculations, we considered $M_{\text{CO}} = 27.995$ amu, $M_{\text{LiF}} = 25.94$ amu, $I_{\text{CO}} = 1.46 \times 10^{-46}$ kg m², and $I_{\text{LiF}} = 3.41 \times 10^{-46}$ kg m². The frequency of the CO stretch vibration was taken to be 269 meV

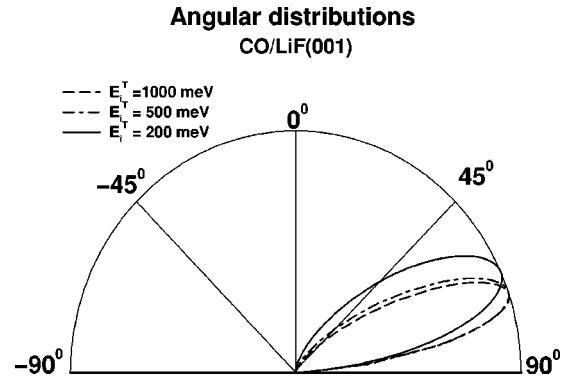


FIG. 2. Angular distributions for the same incident angle and energies as in Fig. 1.

and the polarization vectors appearing in Eq. (16) were calculated from a simple ball-and-spring model, consisting of the O and C molecules connected by a single spring.

The surface temperature is $T_S = 300$ K and the rotational temperature of the incident beam was chosen to be $T_{iR} = 30$ K. The value of the weighted parallel phonon speed was chosen as $v_R = 1000$ m/s, which is consistent with the values used for analyzing the scattering of He atoms¹⁵ and C₂H₂ (Ref. 33) from this same LiF surface. The value of the average angular frequency of frustrated LiF molecular rotations was chosen to be $\omega_R = 2 \times 10^{10}$ s⁻¹, but the value of this parameter is not important because it can be varied by as much as an order of magnitude from this value without significantly affecting the shapes of the curves in Fig. 1. The well depth D is taken to be zero.

The shapes of these energy-resolved spectra are very much similar to those measured for purely atomic beam scattering.³⁴⁻³⁶ For all incident energies, the differential reflection coefficient is a Gaussian-like curve, with the position of maximum intensity at less than one-half of the incident translational energy, indicating a significant energy loss in the scattering process. However, all the curves have a long tail in the high-energy region, and especially at the lower incident energies. This tail extends to energies higher than the incident energy, indicating that a non-negligible fraction of the scattered particles gains energy from the surface. The shapes of these curves being so similar to those often observed for atomic scattering under classical conditions, would indicate that the dominant energy-loss mechanism is to phonons in the collision with the surface. Detailed calculations of the average energy losses to phonons, rotational excitations and to internal excitations confirm this opinion.

B. Angular distributions

Figure 2 shows the angular distributions calculated from Eq. (31) for the same incident conditions as in Fig. 1. In these polar plots the incident angle of $\theta_i = 45^\circ$ is shown as a straight line and the scattered differential reflection coefficients appear as broad lobes in the vicinity of the specular direction. The position of the maximum intensity of these scattered lobes is somewhat greater than the specular angle, and this supraspecular shift increases with incident transla-

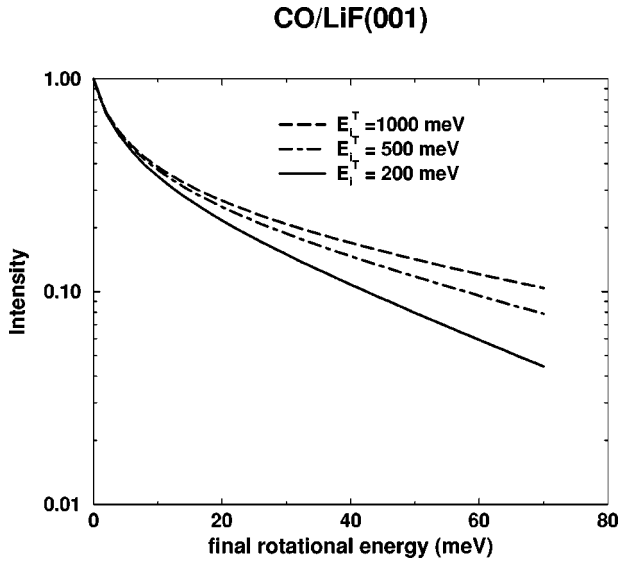


FIG. 3. Scattered intensity versus final rotational energy for CO scattering from LiF(001). The initial angle $\theta_i=45^\circ$, the final angle is, for each incident energy, the position of the maximum in the angular distribution, and $E_i^T=200, 500$, and 1000 meV as marked.

tional energy. The angular distribution also becomes narrower in width with increasing incident energy. These properties are similar to previously observed behavior for atomic beam scattering where the only mechanism for energy exchange is phonon excitation.^{34–36} Again, detailed analysis and breakdown of the three possible modes of energy transfer for the CO molecule indicates that the shapes of the angular distributions are most strongly influenced by phonon exchange.

C. Intensity versus rotational energy

The scattered intensity as a function of the final rotational energy for the scattering of CO from LiF(001) is shown in Fig. 3. The incident energies are again the same as in Fig. 1 and the incident angle is $\theta_i=45^\circ$. The final angle is, for each incident energy, the position of the maximum in the angular distribution (see Fig. 2).

What is plotted here is the differential reflection coefficient of Eq. (29) for fixed incident energy, fixed incident and final angles, averaged over the rotational distribution of the incident beam with a temperature $T_{iR}=30$ K, and finally summed over all other degrees of freedom except for the final rotational energy E_f^R .

What is seen in this semilogarithmic plot is that the intensity falls off very rapidly as a function of E_f^R for the first 10 meV, and then takes on nearly exponentially decreasing behavior as indicated by the curves becoming nearly straight lines. A behavior similar to this has been observed experimentally by Miller and coworkers for the scattering of C_2H_2 from LiF(001) (Ref. 10) under similar conditions of angles and energies. This C_2H_2 experiment did not observe a rapid decay of intensity at very small rotational energies, but the measurements were made only for $E_f^R > 7-9$ meV. Miller and coworkers interpreted their observations as purely expo-

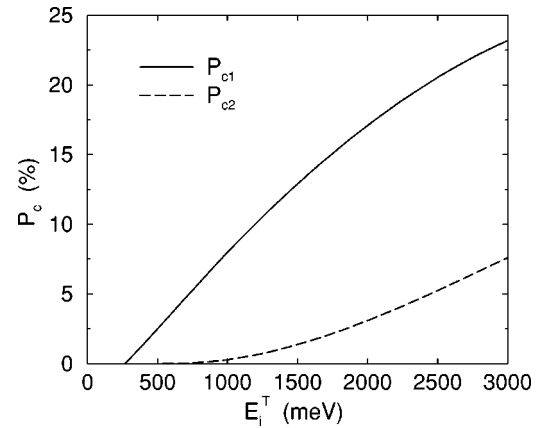


FIG. 4. Excitation probability of the CO internal vibrational mode versus incident translational energy for CO scattering from LiF(001) with an incident angle $\theta_i=45^\circ$. The total probability of the first quantum creation excitation is shown as a solid curve, and the dashed curve is for the second quantum excitation.

ponential decay of the intensity with E_f^R , and through comparison with a Maxwell-Boltzmann distribution, they extracted a final rotational temperature for each incident energy. If a similar interpretation is applied to the curves of Fig. 3 for the straight-line region for $E_f^R > 20$ meV then it is seen that the final rotational temperature increases with increasing incident energy, in qualitative agreement with the observations of Miller and coworkers. The actual values of these final rotational temperatures are 372, 511, and 628 K for $E_i^R=200, 500$, and 1000 meV, respectively.

D. Internal-mode excitation

An example of the excitation probability for the internal molecular mode is shown in Fig. 4. Plotted as a function of the incident translational energy is the fraction of the incident beam (expressed in percent) that is excited into the first and second quantum-excited states ($\alpha=1,2$) of the internal mode. The incident angle is $\theta_i=45^\circ$, the surface temperature is 300 K and the incident beam rotational and vibrational temperatures were set at 30 K and 116 K, respectively, which implies essentially zero excitation probability for the vibrations in the incident beam. It is seen that the total probability for the single quantum excitation, shown as a solid curve, becomes non-negligible for incident energies only slightly higher than the threshold value of $\hbar\omega=269$ meV for the energy of the stretch mode. The double quantum excitation probability, shown as a dashed curve, is not appreciable until approximately four times this incident energy. Triple and higher quantum excitations are negligible at incident energies below 3 eV.

The nearly linear behavior of the $\alpha=1$ excitation probability as a function of E_i^T reflects the biquadratic dependence on momentum exchange \mathbf{p} of the single quantum excitation probability of Eq. (21). The $\alpha=2$ term in the expansion of the full scattering probability of Eq. (20) depends on the product of four factors of \mathbf{p} , and this explains the nearly quadratic behavior of the double quantum excitation probability above its threshold.

IV. CONCLUSIONS

In this paper a theory has been developed for describing the distributions of molecules scattered from a surface illuminated by a well-defined incident molecular beam. This theory is based on a classical-mechanical treatment of the excitation of lattice vibrations upon collision, and a classical-mechanical treatment of rotational transitions of the molecule. The excitation of internal modes of molecular vibration is handled with a quantum-mechanical treatment in the semiclassical limit. This theory should be useful for describing the scattering of molecules having thermal translational velocities or even larger, and having molecular masses significantly larger than hydrogen. Examples of such molecules would be CO, NO, N₂, and CO₂. At thermal velocities such molecules have de Broglie wavelengths significantly shorter than 1 Å, thus a classical treatment of translational motion is adequate. Similarly, rotational quantum numbers of these molecules even at temperatures lower than 100 K are of order 10 or more, and our calculations suggest that the number of rotational quanta that will be exchanged in a typical collision with a surface is also large, thus a classical treatment of the rotation is adequate. However, internal molecular vibrational modes often have large frequencies compared to thermal energies implying that excitation quantum numbers will be small, thus making a fully quantum treatment necessary. In the present case, the theory provides for arbitrary numbers of internal vibrational modes and arbitrarily large quantum excitation numbers for each mode.

The condition for classical-mechanical theory to be valid for describing phonon exchange is that the number of phonons transferred is large. However, for each phonon transferred in surface scattering, linear momentum parallel to the surface is conserved, modulo a surface reciprocal lattice vector. This feature of parallel momentum conservation is important even in the classical multiphonon limit except for the fact that diffraction peaks become densely spaced and all diffraction effects disappear. Linear momentum perpendicular to the surface, on the other hand, is not conserved in phonon transfer due to the broken symmetry normal to the surface. The present theory retains this feature of correct conservation of parallel momentum at a smooth surface. Similarly, for rotational processes, the broken symmetry imposed by the presence of the surface implies that the angular momentum in directions parallel to the surface will not be conserved, but the component perpendicular to the surface will obey a conservation law, and this feature is automatically included in the theory presented here.

The basic result of this theory, as expressed in Eq. (20), is a state-to-state transition rate, which describes a molecule prepared in a well-defined initial momentum, angular momentum, and internal vibrational state to make a transition after collision with a surface to a well-defined final momentum, angular momentum and vibrational state. This theory has a distinct advantage that the fundamental state-to-state transition rate is expressed in closed form as an analytic function. Not only does this make for relatively straightforward calculations, but it provides equations for which the basic physical behavior of the scattering process can readily

be predicted as a function of incident parameters, such as temperatures, energies, and beam angles. Any quantity that can be measured with a detector on the state of the final scattered molecules can readily be calculated from the state-to-state transition rate.

The clarity of the analytic expression of Eq. (20) for the scattered intensities gives physical insight and allows for ready interpretation of the various methods of energy transfer in molecule-surface collisions. The calculations shown in Figs. 1 and 2 indicate that phonon transfers are by far the dominant mechanism for energy transfer. This is evident from Eq. (5), the correlation function for phonon transfer, which is quadratically dependent on the momentum transfer \mathbf{p} . A surface scattering experiment is inherently a back-scattering configuration with large momentum transfers, especially in the direction perpendicular to the surface. These large momentum transfers lead to large probabilities for phonon excitation, just as for the case of scattering of large-mass atomic projectiles. Probabilities for rotational excitation are rather small for a similar reason that they depend on the angular momentum transfer that is relatively small compared to the linear momentum exchange. Also, rotational excitations are suppressed by the large probabilities of phonon excitation, which tends to lead to large translational energy loss and slower final translational velocities. The behavior of internal-mode excitation probabilities is also clearly exhibited in Eq. (20). Both the argument of the modified Bessel function and of the internal-mode contribution to the Debye-Waller factor depend, in the simplest picture, exponentially on the ratio $\mathbf{p}^2/m_j\omega_j$, where ω_j is the mode frequency and m_j is an effective mass for the j th mode, which depends on the mode polarization vectors and is calculated from the normal modes model. For a given scattering configuration, which defines \mathbf{p} , and for the regime of low-excitation probabilities, as encountered here, when the product $m_j\omega_j$ is large the excitation probability for the j -th mode will be small, and vice versa. The interplay between the three modes of energy transfer can also be seen from the form of Eq. (20). For example, the Gaussian-like dependence on energy transfer implies that probabilities for all excitations will tend to be small when the final translational energy is either small or large compared to the incident translational energy. A similar argument implies that choosing a scattering configuration that minimizes the value of the energy transfer term in the Gaussian-like factor is the best condition to observe relatively larger probabilities for rotational- and internal-mode excitations.

Limitations of this theory include the facts that the interaction is strongly repulsive, only phonons are considered as the energy-transfer mechanism to the surface thus neglecting elementary and collective electronic excitations, and the surface is assumed smooth and uncorrugated. Thus in its present form the theory is more applicable to inert surfaces, such as, alkali halides and other insulators, and is less applicable to reactive surfaces, such as metals, where the corrugation of the molecule-surface interaction potential is generally strong and electronic excitations can be important.

A number of improvements to this theory are possible and are in progress. Among these are the inclusion of roughness

and corrugation in the surface, with concomitant multiple collisions of the molecular projectiles with the surface. For describing hyperthermal and higher-energy molecular scattering with metal surfaces it will be necessary to include the additional electronic excitation modes of the surface, such as, electron-hole pairs and both surface and bulk plasmons. Also the form-factor treatment of the interaction used here can be extended to include much more sophisticated models of the interaction potential.

In order to demonstrate the utility of this theory, several representative calculations for the simple diatomic molecule CO scattering from the inert insulator surface LiF(001) were carried out. More extensive calculations and comparison with recent high-precision experiments for the scattering of

C₂H₂ from LiF(001) (Ref. 10) are presented in another paper.³³ There it is shown that this theory can explain measured quantities, such as, angular distributions, scattered intensities as a function of the final rotational energy, and final rotational temperatures as functions of the incident beam energy. Thus it appears that the theoretical approach discussed here can be a useful tool in describing the surface scattering of certain classes of molecules.

ACKNOWLEDGMENTS

This work was supported by the National Science Foundation under Grant No. DMR-0089503 and by the Department of Energy under Grant No. DE-FG02-98ER45704.

-
- ¹E. Watts, G.O. Sitz, D.A. McCormack, G.J. Kroes, R.A. Olsen, J.A. Groeneveld, J.N.P. Van Stralen, E.J. Baerends, and R.C. Mowrey, *J. Chem. Phys.* **114**, 495 (2001).
- ²Elizabeth Watts and Greg O. Sitz, *J. Chem. Phys.* **114**, 4171 (2001).
- ³M.F. Bertino, A.P. Graham, L.Y. Rusin, and J.P. Toennies, *J. Chem. Phys.* **109**, 8036 (1998).
- ⁴Y. Huang, A.M. Wodtke, H. Hou, C.T. Rettner, and D.J. Auerbach, *Phys. Rev. Lett.* **84**, 2985 (2000).
- ⁵H. Hou, Y. Huang, S.J. Gulding, C.T. Rettner, D.J. Auerbach, and A.M. Wodtke, *J. Chem. Phys.* **110**, 10 660 (1999).
- ⁶*Dynamics of Gas-Surface Interactions*, edited by C.T. Rettner and M.N.R. Ashfold (The Royal Society of Chemistry, Cambridge, 1991).
- ⁷D.A. Butler, B. Berenbak, S. Stolte, and A.W. Kleyn, *Phys. Rev. Lett.* **78**, 4653 (1997).
- ⁸A.E. Wiskerke, C.A. Taatjes, A.W. Kleyn, R.J.W.E. Lahaye, S. Stolte, D.K. Bronnikov, and B.E. Hayden, *J. Chem. Phys.* **102**, 3835 (1995).
- ⁹A.C. Wight and R.E. Miller, *J. Chem. Phys.* **109**, 1976 (1998).
- ¹⁰T.W. Francisco, N. Camilone, and R.E. Miller, *Phys. Rev. Lett.* **77**, 1402 (1996).
- ¹¹A.C. Wight and R.E. Miller, *J. Chem. Phys.* **109**, 8626 (1998).
- ¹²A.C. Wight, M. Penno, and R.E. Miller, *J. Chem. Phys.* **111**, 8622 (1999).
- ¹³W. Allison and B. Feuerbacher, *Phys. Rev. Lett.* **45**, 2040 (1980).
- ¹⁴*Helium Atom Scattering from Surfaces*, edited by E. Hulpke, Springer Series in Surface Science (Springer, Berlin, 1992).
- ¹⁵M.F. Bertino, J.R. Manson, and W. Silvestri, *J. Chem. Phys.* **108**, 10 239 (1998).
- ¹⁶V. Bortolani and A.C. Levi, *Riv. Nuovo Cimento* **9**, 1 (1986).
- ¹⁷J.R. Manson, V. Celli, and D. Himes, *Phys. Rev. B* **49**, 2782 (1994).
- ¹⁸R. Brako and D.M. Newns, *Phys. Rev. Lett.* **48**, 1859 (1982).
- ¹⁹R. Brako and D.M. Newns, *Surf. Sci.* **123**, 439 (1982).
- ²⁰H.D. Meyer and R.D. Levine, *Chem. Phys.* **85**, 189 (1984).
- ²¹J.R. Manson, *Phys. Rev. B* **43**, 6924 (1991).
- ²²J.R. Manson, *Phys. Rev. B* **58**, 2253 (1998).
- ²³A. Muis and J.R. Manson, *J. Chem. Phys.* **107**, 1655 (1997).
- ²⁴A. Muis and J.R. Manson, *J. Chem. Phys.* **111**, 730 (1999).
- ²⁵A. Muis and J.R. Manson, *Phys. Rev. B* **54**, 2205 (1996).
- ²⁶J. Dai and J. R. Manson (to be published).
- ²⁷G.D. Mahan, *Many-Particle Physics* (Plenum Press, New York, 1990).
- ²⁸J.R. Manson, *Phys. Rev. B* **37**, 6750 (1988).
- ²⁹H.W. Wyld, *Methods for Physics* (Addison-Wesley, New York, 1993).
- ³⁰V. Celli, G. Benedek, U. Harten, and J.P. Toennies, *Surf. Sci. Lett.* **143**, L376 (1984).
- ³¹H. Zhang and J.R. Manson, *J. Chem. Phys.* **113**, 8290 (2000).
- ³²G.W.C. Kaye and T. H. Laby, *Tables of Physical and Chemical Constants and Some Mathematical Functions* (Longman, London, 1986).
- ³³I. Iftimia and J. R. Manson (unpublished).
- ³⁴W.R. Ronk, D.V. Kowalski, M. Manning, and G.M. Nathanson, *J. Chem. Phys.* **104**, 4842 (1996).
- ³⁵L. Tribe, M. Manning, J.A. Morgan, M.D. Stephens, W.R. Ronk, E. Treptow, G.M. Nathanson, and J.L. Skinner, *J. Phys. Chem.* **102**, 206 (1998).
- ³⁶J.A. Morgan and G.M. Nathanson, *J. Chem. Phys.* **114**, 1958 (2001).